Research Square

Preprints are preliminary reports that have not undergone peer review.
They should not be considered conclusive, used to inform clinical practice,
or referenced by the media as validated information.

Temperature-Dependent Electrical and Interface Properties of Cu/P(VDF-TrFE)-Ho_2O_3/p-Si MPS Structured Schottky Barrier Diodes

Aiswarya K U
Sree Kerala Varma College
K J Arun
drarunkj@gmail.com

Sree Kerala Varma College
M D Aggarwal
Alabama A & M University
Padmaja Guggilla
Alabama A & M University

Research Article

Keywords:

Posted Date: September 8th, 2026

DOI: https://doi.org/10.21203/rs.3.rs-10913597/v1

License: This work is licensed under a Creative Commons Attribution 4.0 International License.
Read Full License

Additional Declarations: No competing interests reported.

Temperature-Dependent Electrical and Interface Properties of Cu/P(VDF-TrFE)-Ho_2O_3/p-Si MPS Structured Schottky Barrier Diodes

Aiswarya K U[1], K J Arun[1]*, M D Aggarwal[2], Padmaja Guggilla[2]

[1]Department of Physics, Sree Kerala Varma College, Thrissur, 680011, Kerala, India.

[2]Department of Physics, Alabama A & M University, Normal, Alabama 35811, USA.

email: drarunkj@gmail.com

Abstract

This work focuses on the preparation of Holmium oxide nanoparticles embedded Polyvinylidene fluoride trifluoroethylene P(VDF-TrFE) as the interfacial insulating layer in the Metal–Polymer–Semiconductor (MPS) structured Schottky Barrier diodes (SBDs). A wet chemical method is used for the synthesis of Ho_2O_3 nanoparticles and a spin-coating technique is used for the preparation of P(VDF-TrFE)/ Ho_2O_3 thin films over silicon wafers. DC sputtering technique is employed to deposit Cu electrode over the thin film forming Cu/ P(VDF-TrFE) - Ho_2O_3/ p-Si MPS structured SBDs. The temperature dependent current–voltage characteristics of the diodes are evaluated by varying the temperature from 30 ºC to 100 ºC. The effect of the P(VDF-TrFE)/ Ho_2O_3 polymer layer on the current–voltage (I-V) characteristics and the performance of the fabricated diode with temperature is discussed. The Capacitance–Voltage (C-V) analysis, together with I-V characteristics, provides a comprehensive understanding of the electrical behavior of the fabricated MIS SBDs and the role of the interfacial layer in controlling charge transport.

Introduction

In recent decades, researchers have shown great interest in the fabrication of metal-semiconductor (MS) type Schottky barrier diodes (SBDs) because of its applications in several optoelectronic and microelectronic devices [1] such as solar cells, photodiodes, gas sensors, transistors and radio-frequency detectors [2-4]. Later researchers incorporated a thin insulator layer between the metal and semiconductor [5] and this changed MS structures into metal-insulator-semiconductor (MIS) structures. Recently, metal–polymer–semiconductor (MPS) structured SBDs have attracted researchers for their stability, low forward voltage drops and fast switching, thus employing them in the areas of sensors [6], thin-film transistors [7], light-emitting diodes [8], Schottky diodes [9, 10] etc. The interfacial layer controls the series resistance, generation–recombination rate of the charge carriers, interface states density, rectification ratio, conduction mechanisms, operation

bandwidth and distribution of the Schottky barrier height and thus affects the performance and reliability of MPS structures [11–15].

Polymer materials have low processing temperatures, high electrical resistivity, high flexibility, light weight, large-area coverage [16–18] which can be utilized in several electronic applications such as energy harvesting, sensors, energy storage, solar cells and light emitting diode (LED) [19]. P(VDF-TrFE) has large polarization, high thermal stability, good piezoelectric, ferroelectric, and pyroelectric properties [20, 21]. P(VDF-TrFE) possesses five crystalline phases which are α, β, γ, δ, and ε [22]. Out of the five phases, β-phase exhibits strongest ferro electric properties due to the spontaneous polarization due to the alignment of parallel dipole of adjacent macro molecular units leading to the formation of zig zag trans (TTTT) conformation [23]. By incorporating suitable nanoparticles in the polymer matrix, an improvement in the optical and electrical properties of polymers are observed due to the interfacial interaction between the polymer and nanoparticles, [24]. Polymer nanocomposites have several applications in the fields of energy harvesters, non-actuators, volatile memory devices, sensors, acoustic transducers, biomedical and electrical devices [25–28]. In this work Holmium oxide nanoparticles are incorporated into P(VDF-TrFE) matrix due to its large band gap, high dielectric constant, good chemical, thermal, mechanical stability and optical properties [29]. They have many applications in the construction of pH sensing films, optical materials, memory devices and wavelength-calibration tools [30–32]. The P(VDF-TrFE)/ Ho_2O_3 is used as the interfacial layer in the fabrication of Cu/ P(VDF-TrFE)- Ho_2O_3/ p-Si SBDs.

Temperature-dependent electrical studies of Cu/ P(VDF-TrFE)- Ho_2O_3/ p-Si SBDs are useful to understand charge transport mechanisms and thermal stability of semiconductor based devices. The electrical characteristics of SBDs are highly temperature dependent, as temperature variations can alter carrier concentration, carrier mobility, thermionic emission process, barrier height and density of interface states [33]. Therefore, investigating the current–voltage characteristics at different temperatures is essential for understanding the dominant conduction mechanisms and the nature of the metal–semiconductor interface. The temperature dependent I-V characteristics of the fabricated MIS Schottky barrier diodes are studied over a suitable temperature range in the present study. The variation in forward and reverse currents is studied for different temperatures and important diode parameters are estimated from the I-V characteristics [34]. In practical, the carrier

transport can be strongly affected by the presence of interface states, defects, localized charges and inhomogeneities in the interfacial layer. The study of these parameters in relation to the temperature thus helps to determine the contribution of the thermally activated transport and interface related effects [35]. The analysis also gives an insight into the thermal stability and reliability of the fabricated devices which are important considerations for their potential application in optoelectronic and photodetection systems.

Experimental

Synthesis of Ho_2O_3 nanoparticles

Holmium oxide (Ho_2O_3) nanoparticles were prepared via a controlled wet chemical precipitation route. In a typical procedure, a 0.05 M aqueous solution of holmium sulfate [$Ho_2(SO_4)_3$] was prepared in triply distilled water under vigorous magnetic stirring. Concurrently, a 0.1 M aqueous solution of sodium hydroxide (NaOH) was introduced dropwise into the precursor solution as the reducing and precipitating agent. The reactive mixture was maintained under continuous stirring for 2 h at a constant temperature of 80 °C to ensure complete precipitation. After cooling to room temperature, the synthesized precipitate was collected via vacuum filtration and washed repeatedly with triply distilled water until all residual ions and reactants were eliminated. The isolated nanostructured powder was dried and subsequently subjected to high-temperature calcination at 1000 °C for 3 h in an electric muffle furnace to obtain highly crystalline Ho_2O_3 nanoparticles.

Preparation of P(VDF-TrFE)/ Ho_2O_3 thin films

Preparation of P(VDF-TrFE)/Ho_2O_3 Nanocomposite Thin Films

The P(VDF-TrFE)/Ho2O3 blend solutions were prepared using a solution-casting technique. Initially, 500 mg of Polyvinylidene fluoride-trifluoroethylene [P(VDF-TrFE)] copolymer powder was dissolved in 20 mL of N, N-dimethyl formamide (DMF) solvent. This solution was continuously stirred at 60 °C for 2 h until a completely homogeneous, transparent polymer matrix was obtained. Subsequently, pre-weighed portions of the calcined Ho2O3 nanoparticles were added to separate polymer solutions to achieve target filler weight fractions of 6 wt%, 8 wt%, and 10 wt%. The resulting suspensions were stirred vigorously at 60 °C for an additional 2 h to induce uniform nanoparticle dispersion and minimize phase separation. For baseline surface morphology screening, the solutions were spin-coated onto meticulously cleaned glass substrates at 2000 rpm

for 30 s and subsequently soft-baked at 60 °C for 2 h to evaporate the residual DMF solvent. The optimized composite thin film configurations were designated as HO6 (6 wt%), HO8 (8 wt%), and HO10 (10 wt%), respectively.

Fabrication of Cu/ P(VDF-TrFE)- Ho_2O_3/ p-Si SBDs

Fabrication of Cu/P(VDF-TrFE)-Ho2O3/p-Si MPS Structured SBDs

To fabricate the Metal-Polymer-Semiconductor (MPS) Schottky barrier diodes, single-crystal p-type Silicon (p-Si) wafers were utilized as the semiconductor base substrates. The p-Si wafers were chemically cleaned to eliminate native oxides and organic contaminants. The prepared P(VDF-TrFE)/Ho_2O_3 solutions (HO6, HO8, and HO10) were directly spin-coated onto the active front surface of the cleaned p-Si wafers at 2000 rpm for 30 s, followed by a thermal bake at 60°C for 2 h to produce uniform, pinned interfacial insulating thin layers. To form the Schottky front contacts, a high-purity Copper (Cu) metal layer was deposited over the P(VDF-TrFE)-Ho_2O_3/p-Si heterostructures via DC magnetron sputtering (HIND High Vacuum-BC 300 system). The top contact deposition was performed through a shadow mask to define structured, isolated Cu macro-electrodes. The final Cu/P(VDF-TrFE)-Ho2O3/p-Si MPS SBD architectures were cured at room temperature prior to executing systematic temperature-resolved electrical characterizations.

Results and discussions

Atomic force microscopy (AFM) analysis

Atomic force microscopy (AFM) is employed to investigate the surface morphology and roughness characteristics of Ho_2O_3-incorporated P(VDF-TrFE) nanocomposite films as shown in Fig. 1. The AFM topography (3D) reveals a relatively smooth and continuous surface with gently undulating features, indicating uniform dispersion of Ho_2O_3 nanoparticles within the polymer matrix due to the good interfacial compatibility between Ho_2O_3 and P(VDF-TrFE). The calculated RMS values are 66, 53 and 51 nm for HO6, HO8 and HO10. It indicates that as loading percentage of nanoparticles increases, smoothness and compactness of the films also increase. This RMS values confirms the formation of a uniform film layer will favor the diode fabrication [36]. Prior reports by C.V. Prasad et.al, P.P. Thapaswini et.al and V.R. Reddy et.al, reported that samples with fairly smooth surface showed better diode performance [37, 38] by improving the rectifying nature of MIS junction and Schottky diode parameters. The strong polymer-nanoparticle interfacial

interaction exists as the nanoparticles fill the free voids between polymer chains thereby making the polymer chains more ordered or constrained. The AFM analysis demonstrates that Ho_2O_3 concentration plays a crucial role in determining the surface morphology of P(VDF-TrFE) thin films. Among the investigated compositions, the HO10 film exhibits the most favorable surface characteristics, with reduced roughness and homogeneous morphology, indicating optimal nanoparticle dispersion [39]. Excessive Ho_2O_3 loading leads to agglomeration and increased height variation, highlighting the existence of an optimal filler concentration for achieving uniform surface morphology and improved functional performance. The uniform, smooth topography recorded for the HO10 optimal configuration suppresses localized electric field spikes and spatial defects, paving the way for consistent interfacial potential profiles that drastically improve the rectifying parameters of the fabricated MIS Schottky junctions.

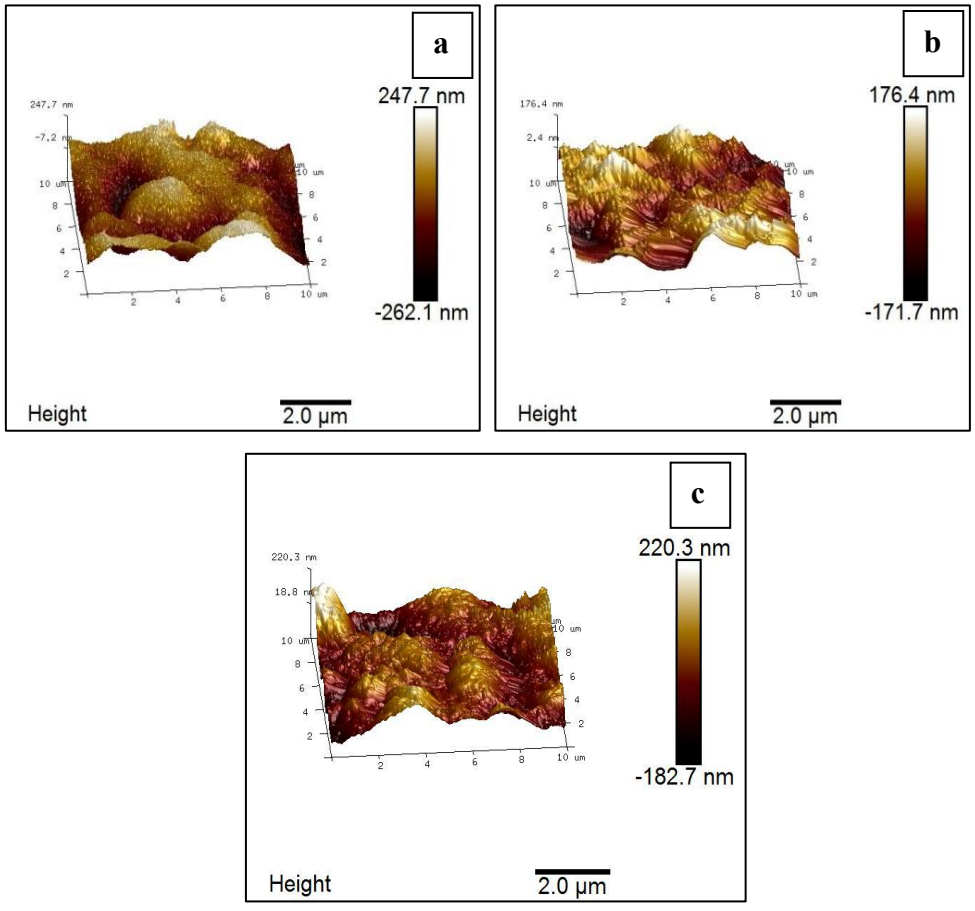


Fig. 1 AFM images of (a) HO6 (b) HO8 (c) HO10

I-V characterization of Cu/ P(VDF-TrFE)- Ho_2O_3/ p-Si Schottky barrier diodes with temperature variation

Fig. 2 shows the I-V characteristics of fabricated diodes measured using Keithley source meter by varying temperature from 30˚C to 100˚C in the voltage range - 5 V to 5 V and explores how the temperature variations influence the I-V characteristics of the MPS diodes. It is observed that the current increases with the applied voltage and temperature. As the temperature increases, the number of thermally excited carriers increases to overcome the potential barrier, leading to a higher current flow [40]. A diode must perform reliably over a temperature range, otherwise its performance may degrade. The plot of ln J versus V is shown in Fig. 3. TE theory is employed in the evaluation of the current density (J) as given by the equations (1-2)

$$J = J_0 \left[\exp\left(\frac{qV}{nk_BT}\right) - 1\right] \quad (1)$$

$$J_0 = A^*T^2 \exp\left(-\frac{q\Phi_B}{k_BT}\right) \quad (2)$$

Where J_0, q, V, n, k_B, A*, T and Φ_B are reverse leakage current density, electron charge, voltage applied, ideality factor, Boltzmann's constant, Richardson constant (32 A/cm^2K^2 for p-Si), temperature in kelvin and effective barrier height. The ideality factor (n) and barrier height (Φ_B) can be calculated by the following equations (3-4) [41]

$$n = \frac{q}{k_BT}\left(\frac{dV}{d(\ln J)}\right) \quad (3)$$

$$\Phi_B = \frac{k_BT}{q}\ln\left(\frac{A^*T^2}{J_0}\right) \quad (4)$$

Temperature variations can affect the effective barrier height and the ideality factor of MPS diodes. The temperature dependent values of ideality factor and barrier height determined from equations 3 and 4 are given in Table. 1. The temperature dependence of the ideality factor and barrier height for Cu/ P(VDF-TrFE)- Ho_2O_3/ p-Si type SBDs is shown in Fig. 4.

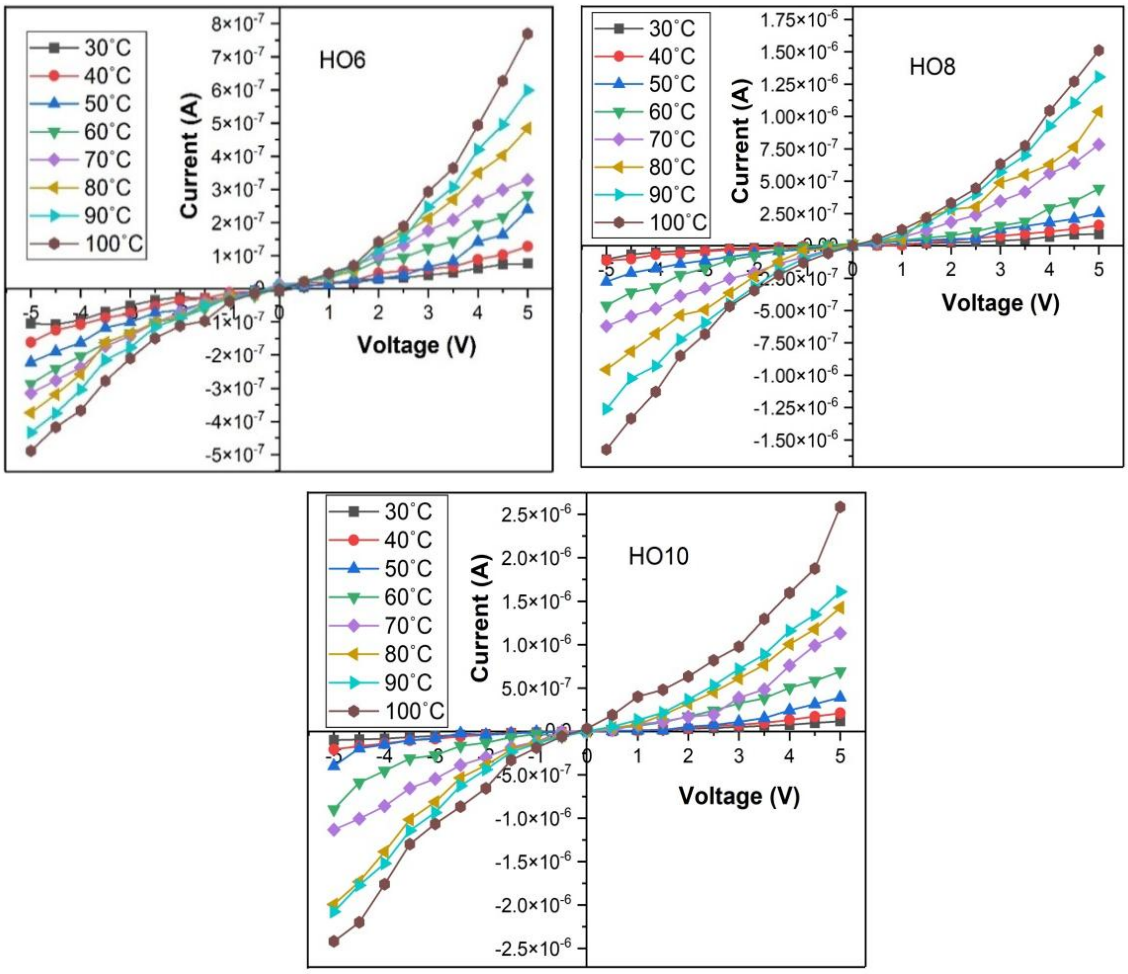


Fig. 2 I-V characteristics of the Cu/ P(VDF-TrFE)- Ho_2O_3/ p-Si SBDs at different temperatures

A number of factors, including interface states, high series resistance, charge recombination within the space charge region and imperfections in the insulating layer, cause deviations from the ideality factor, which should be near 1 [42]. The majority of metal-insulator-semiconductor (MIS) diodes have n=1, indicating that the TE mechanism is predominant. Other transport processes such as tunneling, recombination and trap-assisted conduction may occur when n exceeds 1. As the temperature rises from 30˚C to 100˚C, the barrier height increases from 0.653 eV to 0.681 eV and the ideality factor decreases from 5.33 to 3.89 for HO10. In MPS diodes, the current conduction is a temperature-activated process [43]. Electrons can only pass through lower barriers at lower temperatures. Electrons acquire sufficient energy to get past high barriers at high temperatures [44]. Due to surface inhomogeneity in the Schottky contact interface, numerous researchers have

documented an increase in barrier height and a decrease in ideality factor with temperature [45]. Both n and Φ_B are typically temperature independent for an ideal Schottky diode. The lack of a pure TE mechanism in the diodes is evident from the temperature dependence of the n and Φ_B values [46]. The barrier inhomogeneities resulting from the non-uniform interfacial layer and the non-uniform charge distribution between the Cu and p-Si are the primary causes of the diode's departure from the pure TE mechanism [47].

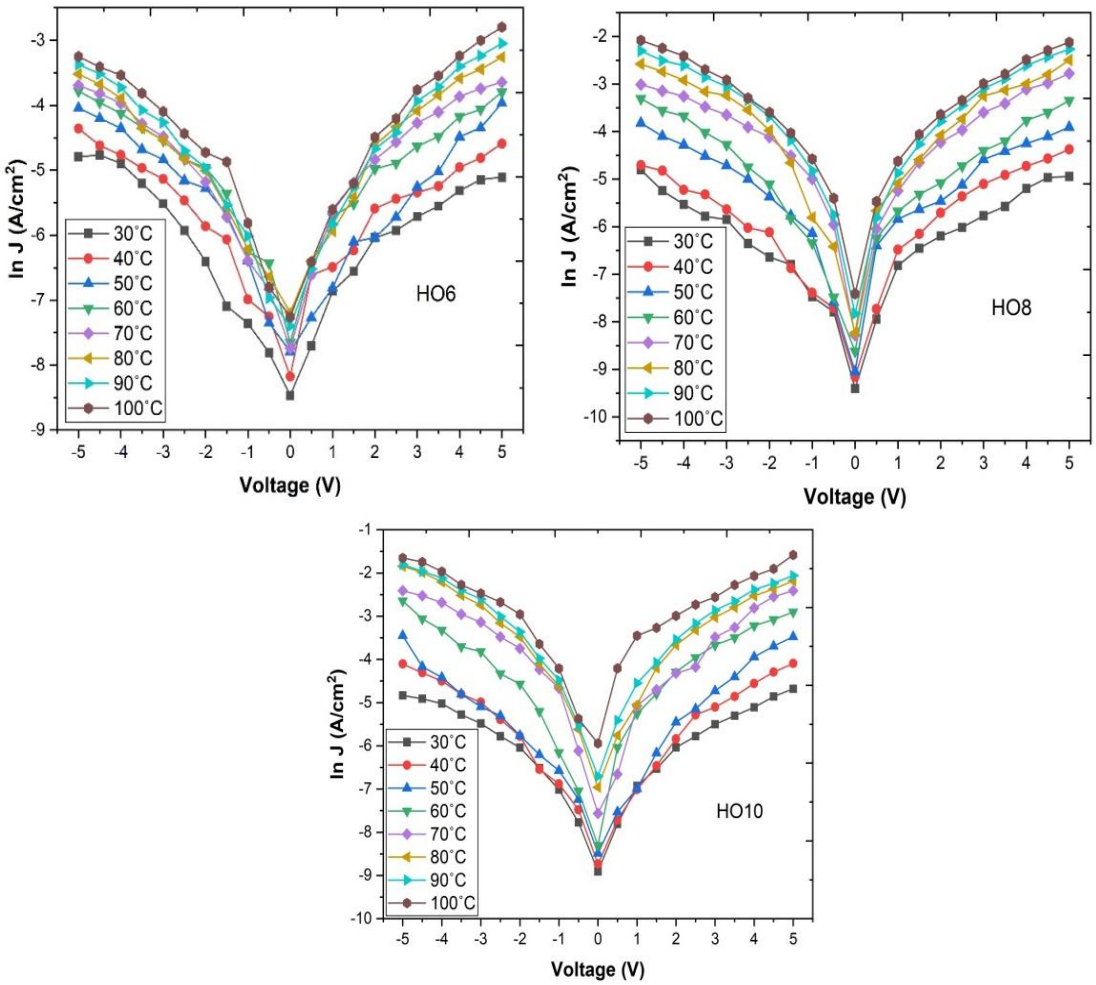


Fig. 3 Temperatures dependent ln (J)-V plots for Cu/ P(VDF-TrFE)- Ho_2O_3/ p-Si SBDs

Temperature (˚C)	Ideality factor (n)			Barrier height eV (Φ_B)		
	HO6	HO8	HO10	HO6	HO8	HO10
30	5.52	5.42	5.33	0.648	0.651	0.653
40	5.36	5.20	5.13	0.650	0.658	0.660
50	5.24	5.08	4.75	0.653	0.662	0.663
60	5.17	4.80	4.56	0.658	0.664	0.666
70	4.69	4.64	4.38	0.660	0.668	0.671
80	4.37	4.30	4.22	0.664	0.670	0.675
90	4.26	4.19	4.15	0.668	0.672	0.678
100	4.13	4.09	3.89	0.672	0.674	0.681

Table. 1 Diode parameters of Cu/ P(VDF-TrFE)- Ho_2O_3/ p-Si SBDs at different temperatures

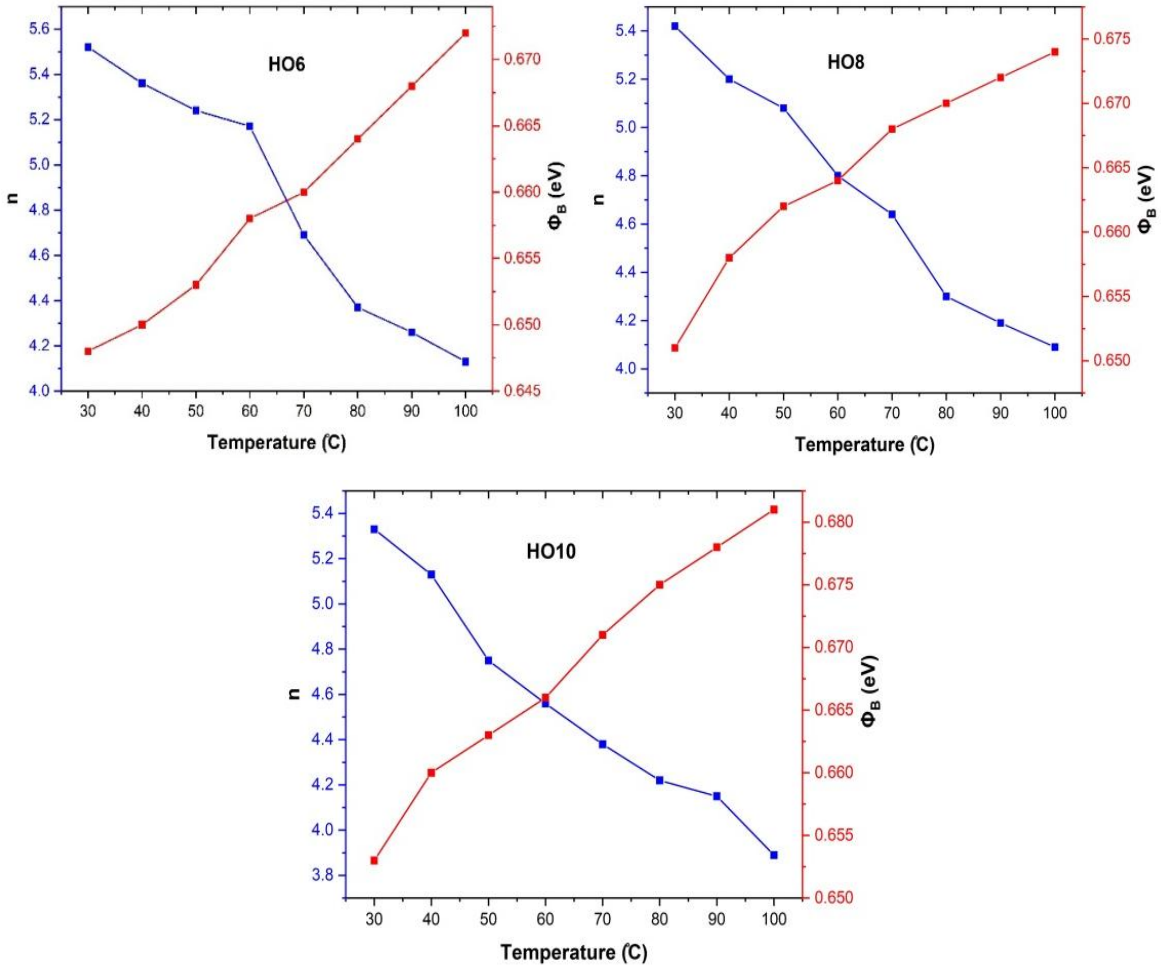


Fig. 4 Temperature dependent variation of n and Φ_B for Cu/ P(VDF-TrFE)- Ho_2O_3/ p-Si SBDs

Capacitance-Voltage characteristics of Cu/ P(VDF-TrFE)- Ho_2O_3/ p-Si diodes

The C-V characteristics of the Cu/ P(VDF-TrFE)- Ho_2O_3/ p-Si diodes at room temperature measured under a frequency of 1 MHz using a Key sight E4990A impedance analyzer is presented in Fig. 5. The contribution to the capacitance due to interface traps is negligible at high frequencies and hence the frequency of 1 MHz is chosen for the study of C-V profile. There is roughly no variation of capacitance with voltage in the reverse bias voltage range. However, in the forward bias range, a sudden increase in capacitance with voltage is seen [48]. The increase in capacitance at positive voltages depending on the bias indicates a strong interfacial (Maxwell-Wagner) polarization at the nanoparticle-polymer interfaces.

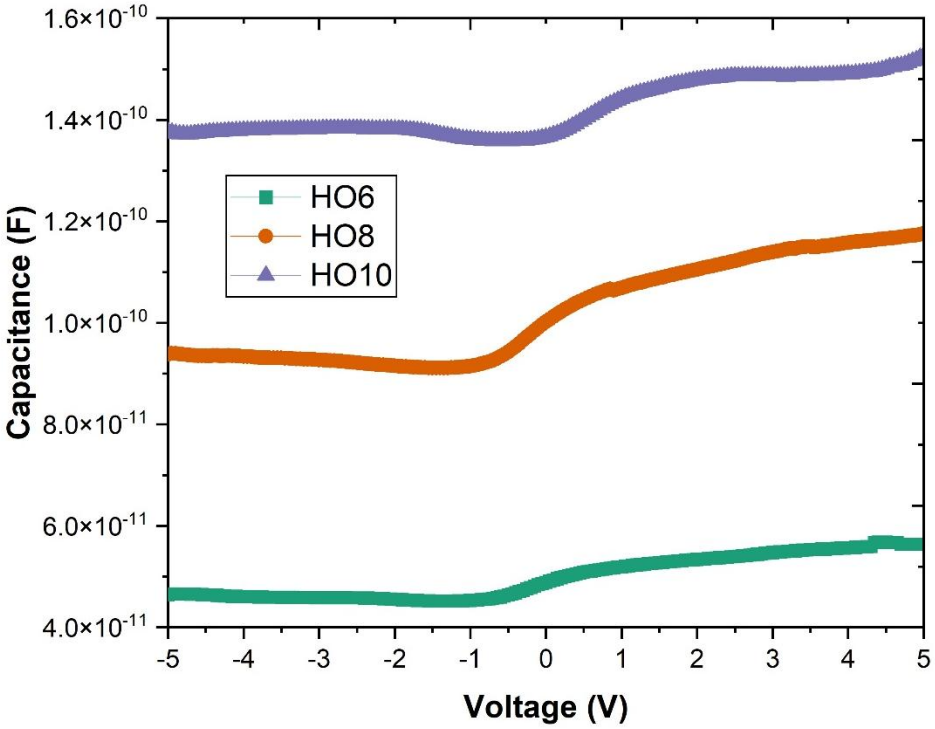


Fig. 5 C-V characteristics of Cu/ P(VDF-TrFE)- Ho_2O_3/ p-Si MPS structured SBDs

Fig. 6 shows the C^{-2}-V plot from which the barrier height can be evaluated using the following equation [49]

$$\Phi_B = V_d + \frac{kT}{q} \ln\left(\frac{N_V}{N_A}\right) \quad (5)$$

Where V_d is defined as the diffusion potential. The origin of the kT/q term is based on the effect of the penetration of electrons from the metal to the depletion region [50]. N_A can be calculated

from the slope of the C^{-2}-V plot. $N_V = 1.04 \times 10^{19}$ cm^{-3} is the effective density of states in the Si valence band. The parameters obtained from the C^{-2}-V characteristics are given in Table. 2. The barrier height values obtained from I-V method and C-V method are close to each other. When the interface is clean and has very few interface states or oxide defects, both the I-V and C-V methods give almost the same potential barrier. By using relatively thick depletion layers, image-force barrier lowering and tunneling are suppressed so that the effective transport barrier (I-V) is not reduced with respect to the electrostatic barrier (C-V).

Sample	**V_d (V)**	**N_A (cm^{-3})**	**Φ_B (I-V method at 30°C)**	**Φ_B (C-V method)**
HO6	0.528	2.105×10^{19}	0.648	0.509
HO8	0.594	5.789×10^{18}	0.651	0.605
HO10	0.638	1.116×10^{18}	0.653	0.696

Table. 2 The parameters obtained from the C^{-2}-V characteristics of SBDs

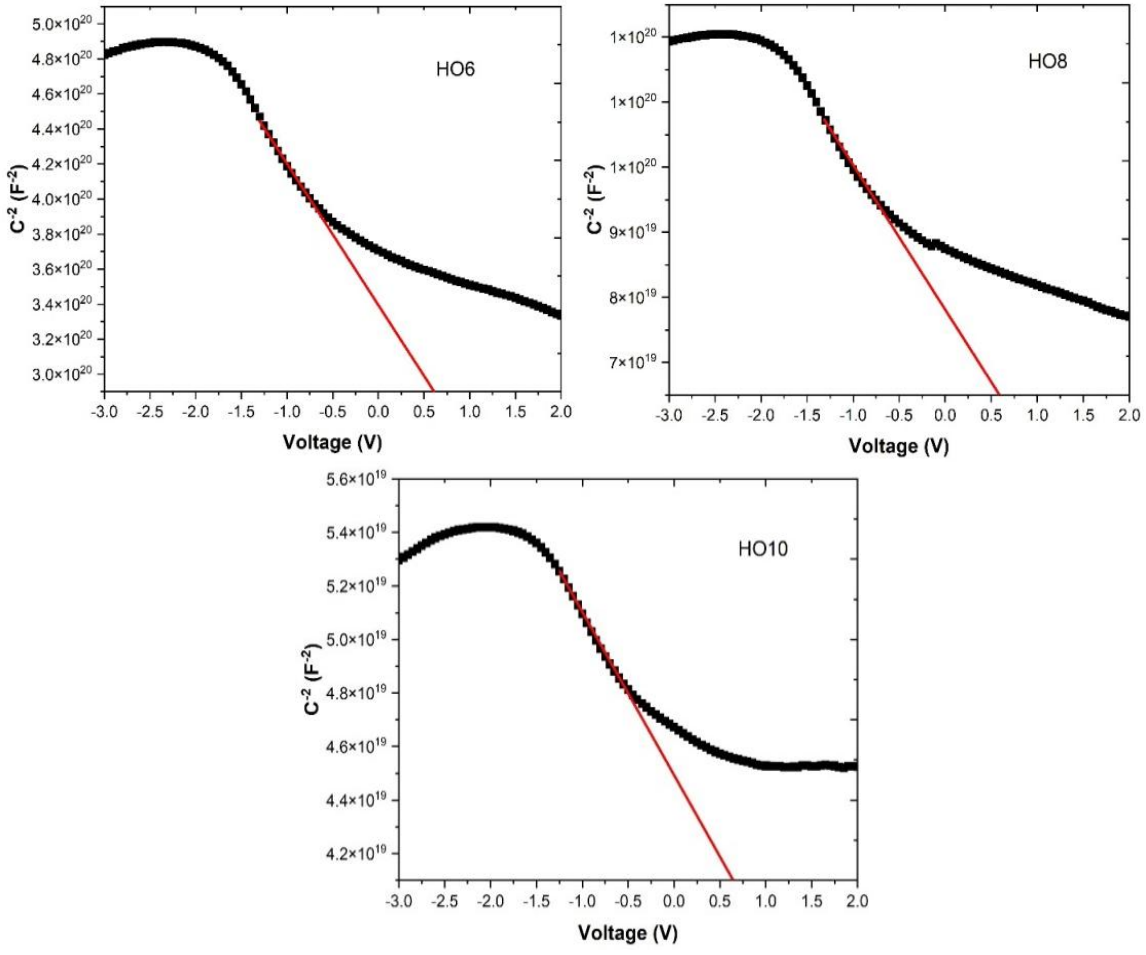


Fig. 6 C^{-2}-V plots of Cu/ P(VDF-TrFE)- Ho_2O_3/ p-Si MPS structured SBDs

Conclusions

A high-performance Cu/ P(VDF-TrFE)- Ho_2O_3/ p-Si Schottky Barrier diodes were fabricated with different concentration of Ho_2O_3 in P(VDF-TrFE) matrix using Spin coating technique. The temperature dependent I-V performances of the diodes were evaluated by varying the temperature from 30˚C to 100˚C. The I-V characteristics measured over the investigated temperature range revealed a significant increase in forward current with increasing temperature. The extracted diode parameters exhibited a noticeable dependence on temperature. A decrement in the ideality factor and an increment in the barrier height with temperature was observed. The temperature-dependent studies demonstrate that the electrical transport in the fabricated MIS Schottky barrier diodes is governed by a combination of thermally activated carrier transport and interface-related effects The results provide useful information regarding the stability, charge transport behavior, and interfacial properties of the devices. Such an understanding is essential for optimizing the interfacial layer and improving the performance and reliability of MIS Schottky barrier diodes. The comprehensive findings demonstrate that blending Ho_2O_3 nanoparticles into a P(VDF-TrFE) matrix produces a thermally stable, high-k interfacial layer capable of regulating charge transport, which provides valuable design parameters for optimizing reliable, high-performance MIS-type microelectronic and optoelectronic switching devices.

Acknowledgements

The authors acknowledge UGC, DST-FIST and KSCSTE for the support in setting up of facilities for research at Sree Kerala Varma College, Thrissur. Author Aiswarya K.U likes to thank Kerala State Council for Science Technology and Environment, Government of Kerala for awarding a research fellowship grant.

Author contributions

All the authors have accepted responsibility for the entire content of this submitted manuscript and approved submission.

K J Arun: Conceptualization, Methodology, investigation, supervision, Writing- Original draft preparation, editing, reviewing, validation. **Aiswarya K U**: Data curation, Writing- Original draft preparation, software, investigation. **M D Aggarwal**: Visualization, Software, Validation, Reviewing. **Padmaja Guggilla**: Visualization, Reviewing, Validation.

Declarations

Competing Interests

No, I declare that the authors have no competing interests as defined by Discover, or other interests that might be perceived to influence the results and/or discussion reported in this paper.

Dual Publication

The results/data/figures in this manuscript have not been published elsewhere, nor are they under consideration (from you or one of your Contributing Authors) by another publisher.

Authorship

I have read the Nature Portfolio journal policies on author responsibilities and submit this manuscript in accordance with those policies.

Third Party Material

All of the material is owned by the authors and/or no permissions are required.

Data Availability

Yes, I have research data to declare.

“The datasets generated during and/or analyzed during the current study are available from the corresponding author on reasonable request.”

Research Funding

This research did not receive funding.

Ethics approval and consent to participate

Not applicable.

Consent for publication

Not applicable.

References

1. Tung, R. T., J. P. Sullivan, and F. Schrey, On the inhomogeneity of Schottky barriers, Materials Science and Engineering: B. 14, no. 3 (1992) 266-280., https://doi.org/10.1016/0921-5107 (92)90309-W.
2. Naama, S., T. Hadjersi, A. Keffous, and G. Nezzal, CO_2 gas sensor based on silicon nanowires modified with metal nanoparticles, Materials Science in Semiconductor Processing. 38 (2015) 367-372. https://doi.org/10.1016/j.mssp.2015.01.027.
3. Vittal, R., and Kuo-Chuan Ho, Zinc oxide based dye-sensitized solar cells: A review, Renewable and Sustainable energy reviews. 70 (2017) 920-935. https://doi.org/10.1016/j. rser.2016.11.273.
4. Dökme, İlbilge, Tuncay Tunç, İbrahim Uslu, and Şemsettin Altındal, The Au/polyvinyl alcohol (Co, Zn-doped)/n-type silicon Schottky barrier devices, Synthetic metals. 161, no. 5-6 (2011) 474-480. https://doi.org/10.1016/j.synthmet.2011.01.002.
5. Willars-Rodríguez, F. J., I. R. Chávez-Urbiola, R. Ramírez-Bon, P. Vorobiev, and Yu V. Vorobiev. Effects of aluminum doping in CdS thin films prepared by CBD and the performance on Schottky diodes TCO/CdS: Al/C, Journal of Alloys and Compounds. 817 (2020) 152740. https://doi.org/10.1016/j.jallcom.2019.152740.
6. Tunç, Tuncay, İbrahim Uslu, İlbilge Dökme, Şemsettin Altındal, and Habibe Uslu, Frequency and temperature dependence of dielectric properties of Au/polyvinyl alcohol (Co, Ni-doped)/n-Si Schottky diodes, International Journal of Polymeric Materials. 59, no. 10 (2010) 739-756. https://doi.org/10.1080/00914037.2010.483215.
7. Yakuphanoglu, Fahrettin, Controlling of silicon–insulator–metal junction by organic semiconductor polymer thin film, Synthetic metals. 160, no. 13-14 (2010) 1551-1555. https://doi.org/10.1016/j.synthmet.2010.05.024.
8. Tamilavan, Vellaiappillai, Pachagounder Sakthivel, Yinan Li, Myungkwan Song, Chul-Hyun Kim, Sung-Ho Jin, and Myung Ho Hyun, Synthesis and characterization of indenofluorene-based copolymers containing 2, 5-bis (2-thienyl)-N-arylpyrrole for bulk

heterojunction solar cells and polymer light-emitting diodes, Journal of Polymer Science Part A: Polymer Chemistry. 48, no. 14 (2010) 3169-3177. https://doi.org/10.1002/pola.24101.

9. Kwon, Jun Ho, Ji-Young An, Hanmae Jang, Solji Choi, Dae Sung Chung, Min-Jung Lee, Hyo-Jung Cha, Jin-Hee Park, Chan-Eon Park, and Yun-Hi Kim, Development of a new conjugated polymer containing dialkoxynaphthalene for efficient polymer solar cells and organic thin film transistors, Journal of Polymer Science Part A: Polymer Chemistry. 49, no. 5 (2011) 1119-1128. https://doi.org/10.1002/pola.24526.
10. Du, J. F., Y. Bai, W. Y. Chu, and L. J. Qiao, The microstructure and performance of solid-state hydrogen sensor using CH_3COONH_4-doped chitosan as electrolyte, Journal of Applied Electrochemistry. 41, no. 2 (2011) 183-187. https://doi.org/10.1007/s10800-010-0222-7.
11. Demirezen, Selçuk, and Seçkin Altındal Yerişkin, A detailed comparative study on electrical and photovoltaic characteristics of Al/p-Si photodiodes with coumarin-doped PVA interfacial layer: the effect of doping concentration, Polymer Bulletin. 77, no. 1 (2020) 49-71. https://doi.org/10.1007/s00289-019-02704-3.
12. Tozlu, Cem, and Adem Mutlu, Poly (melamine-co-formaldehyde) methylated effect on the interface states of metal/polymer/p-Si Schottky barrier diode, Synthetic Metals. 211 (2016) 99-106. https://doi.org/10.1016/j.synthmet.2015.11.023.
13. Boughdachi, S., Y. O. S. E. F. Badali, Y. A. S. H. A. R. Azizian-Kalandaragh, and Ş. Altındal, Current-Transport Mechanisms of the Al/(Bi_2S_3-PVA Nanocomposite)/p-Si Schottky Diodes in the Temperature Range Between 220 K and 380 K: Boughdachi, Badali, Azizian-Kalandaragh, and Altındal, Journal of Electronic Materials. 47, no. 12 (2018): 6945-6953. https://doi.org/10.1007/s11664-018-6593-y.
14. Mousavi, Seyedeh Soraya, Batool Sajad, and Mohammad Hossein Majlesara, Fast response ZnO/PVA nanocomposite-based photodiodes modified by graphene quantum dots, Materials & Design. 162 (2019) 249-255. https://doi.org/10.1016/j.matdes.2018.11.037.
15. Badali, Yusuf, Yashar Azizian-Kalandaragh, İbrahim Uslu, and Şemsettin Altindal, Investigation of the effect of different Bi_2O_3–x: PVA (x= Sm, Sn, Mo) thin insulator

interface-layer materials on diode parameters, Journal of Materials Science: Materials in Electronics. 31, no. 10 (2020) 8033-8042. https://doi.org/10.1007/s10854-020-03343-5.

16. Yuan, Yongbo, Timothy J. Reece, Pankaj Sharma, Shashi Poddar, Stephen Ducharme, Alexei Gruverman, Yang Yang, and Jinsong Huang, Efficiency enhancement in organic solar cells with ferroelectric polymers, Nature materials. 10, no. 4 (2011) 296-302. https://doi.org/10.1038/nmat2951.
17. Li, Mengyuan, Ilias Katsouras, Claudia Piliego, Gunnar Glasser, Ingo Lieberwirth, Paul WM Blom, and Dago M. de Leeuw, Controlling the microstructure of poly (vinylidene-fluoride)(PVDF) thin films for microelectronics, Journal of Materials Chemistry C. 1, no. 46 (2013) 7695-7702.https://doi. org/10.1039/C3TC31774A.
18. Li, Baozhang, Chengyi Xu, Feifei Zhang, Jianming Zheng, and Chunye Xu, Self-polarized piezoelectric thin films: preparation, formation mechanism and application, Journal of Materials Chemistry C. 3, no. 34 (2015) 8926-8931. https://doi. org/10.1039/C5TC01869B
19. Groh, W., and A. Zimmermann, What is the lowest refractive index of an organic polymer, Macromolecules. 24, no. 25 (1991) 6660-6663. https://doi.org/10.1021/ma00025a016.
20. Ghule, Babaji, Meena Laad, Girish Kale, and Kishor Kumar Sadasivuni, Polymer nanocomposite film and coating for electronic and optoelectronic devices, In Polymer Nanocomposite Films and Coatings (2024) 293-331. Woodhead Publishing. https://doi.org/10.1016/ B978-0-443-19139-8.00016-4.
21. Peng, Ruobo, Butong Zhang, Guohua Dong, Yinghui Wang, Guannan Yang, Jie Zhang, Bin Peng, Yanan Zhao, and Ming Liu, Enhanced piezoelectric energy harvester by employing freestanding single-crystal $BaTiO_3$ films in PVDF-TrFE based composites, Advanced Functional Materials. 34, no. 27 (2024) 2316519. https://doi.org/10.1002/adfm.202316519.
22. Nanda, K. K., S. N. Sarangi, S. Mohanty, and S. N. Sahu, Optical properties of CdS nanocrystalline films prepared by a precipitation technique, Thin Solid Films. 322, no. 1-2 (1998) 21-27. https://doi. org/10.1016/S0040-6090(97)01015-8.
23. Li, Qi, and Qing Wang, Ferroelectric polymers and their energy-related applications, Macromolecular Chemistry and Physics. 217, no. 11 (2016) 1228-1244. https://doi.org/10.1002/macp.201500503.

24. Sun, Yipeng, Encai Hao, Xi Zhang, Bai Yang, Jiacong Shen, Lifeng Chi, and Harald Fuchs, Buildup of composite films containing TiO_2/PbS nanoparticles and polyelectrolytes based on electrostatic interaction, Langmuir. 13, no. 19 (1997) 5168-5174. https://doi.org/10.1021/la9703510.
25. Aiswarya, K. U., K. J. Arun, and M. D. Aggarwal, Calcination tuned structural, optical and dielectric properties of wet chemically synthesised cadmium tungstate nanoparticles for photocatalytic and photodetector applications, New Journal of Chemistry. 49, no. 42 (2025) 18479-18492. https://doi.org/10.1039/d5nj03272e.
26. Dagdeviren, Canan, Pauline Joe, Ozlem L. Tuzman, Kwi-Il Park, Keon Jae Lee, Yan Shi, Yonggang Huang, and John A. Rogers, Recent progress in flexible and stretchable piezoelectric devices for mechanical energy harvesting, sensing and actuation, Extreme mechanics letters. 9 (2016) 269-281. https:// doi.org/10.1016/j.eml.2016.05.015.
27. Aiswarya, K. U., K. J. Arun, and M. D. Aggarwal, Wet chemical synthesis optimisation and characterisation of nano holmium oxide for photocatalytic and dielectric device applications, Surface Engineering and Applied Electrochemistry. 61, no. 1 (2025) 12-23. https://doi.org/10.3103/S1068375524700522.
28. Ansari, Parveen, Kamal Kumar Kushwah, Muni Raj Maurya, Mithra Geetha, Kishor Kumar Sadasivuni, Hussain Jeevakhan, Shilpi Jindal, and Meera Ramrakhaini, Opto-mechanical studies of PVA-capped ZnSe and CdSe nanoparticles for optoelectronic applications, Bulletin of Materials Science. 47, no. 1 (2024) 43. https:// doi.org/10.1007/s12034-023-03122-y.
29. Gasgnier, M, Rare earth compounds (oxides, sulfides, silicides, boron,...) as thin films and thin crystals (1989) 11-71. https://doi.org/10.1002/pssa.2211140102.
30. T. Wiktorczyk, Preparation and optical properties of holmium oxide thin films, Thin Solid Films. 405 (2002) 238–242. https://doi.org/10.1016/S0040-6090(01) 01760-6.
31. Timur Sh Atabaev, Yong Cheol Shin, Su-Jin Song, Dong-Wook Han, Nguyen Hoa Hong, Toxicity and T_2-weighted magnetic resonance imaging potentials of holmium oxide nanoparticles, Nanomaterials. 7 (2017) 216. https://doi.org/ 10.3390/nano7080216.
32. Bahaa M. Abu-Zied, Abdullah M. Asiri, Genesis of nanocrystalline Ho_2O_3 via thermal decomposition of holmium acetate: structure evolution and electrical conductivity properties, J. Rare Earths. 37 (2019) 185–192. https://doi.org/ 10.1016/j.jre.2018.05.017.

33. KU, Aiswarya, K. J. Arun, and M. D. Aggarwal, Investigations on the current conduction mechanism in PVA-$CdWO_4$ films and the temperature-dependent electrical characteristics of Cu/(PVA-$CdWO_4$)/p-Si metal–polymer–semiconductor diodes, Journal of Physics D: Applied Physics. 58, no. 41 (2025) 415109. https://doi.org/10.1088/1361-6463/ae0a66.
34. Aiswarya, K. U., K. J. Arun, M. D. Aggarwal, R. Marnadu, and Pius Augustine, Dielectric studies, ferroelectric behaviour and electronic transport mechanisms in β phase enhanced P (VDF-TrFE)/Ho_2O_3 films for possible energy storage applications, Measurement: Energy. 6 (2025) 100046. https://doi.org/10.1016/j.meaene.2025.100046.
35. Arun, K. J., and M. D. Aggarwal, Fabrication and characterization of illumination-dependent Cu/p-Si Schottky barrier diodes with P (VDF-TrFE)-Ho_2O_3 nano composite as interfacial insulating layer, Emergent Materials. 8, no. 5 (2025) 3853-3864. https://doi.org/10.1007/s42247-024-00897-6.
36. Prasad, C. Venkata, M. Siva Pratap Reddy, V. Rajagopal Reddy, Chinho Park, Effect of annealing on chemical, structural and electrical properties of Au/Gd_2O_3/n-GaN heterostructure with a high-k rare-earth oxide interlayer, Applied Surface Science. 427 (2018) 670-677. https://doi.org/10.1016/j.apsusc.2017.09.016.
37. Thapaswini, P. Prabhu, R. Padma, N. Balaram, B. Bindu, V. Rajagopal Reddy, Modification of electrical properties of Au/n-type InP Schottky diode with a high-k $Ba_{0.6}Sr_{0.4}TiO_3$ interlayer, Superlattices and Microstructures. 93 (2016) 82-91. https://doi.org/10.1016/j.spmi.2016.03.010.
38. Rajagopal Reddy, V., V. Manjunath, V. Janardhanam, Yeon-Ho Kil, Chel-Jong Choi, Electrical properties and current transport mechanisms of the Au/n-GaN Schottky structure with solution-processed high-k $BaTiO_3$ interlayer, Journal of electronic materials. 43, no. 9 (2014) 3499-3507. https://doi.org/10.1007/s11664-014-3177-3.
39. Aiswarya, K. U., K. J. Arun, and M. D. Aggarwal, Fabrication and characterisation of high response Cu/(PVA-$CdWO_4$)/p-Si Schottky diode for ultraviolet photo detection, Current Applied Physics (2025). https://doi.org/10.1016/j.cap.2025.09.008.
40. Perez, Gaëtan, Gauthier Chicot, Yvan Avenas, Pierre Lefranc, Pierre-Olivier Jeannin, David Eon, Nicolas Rouger, Integrated temperature sensor with diamond Schottky diodes using a thermosensitive parameter, Diamond and Related Materials. 78 (2017) 83-87. https://doi.org/10.1016/j.diamond.2017.08.008.

41. Uma, M., N. Balaram, P. R. Sekhar Reddy, V. Janardhanam, V. Rajagopal Reddy, Hyung-Joong Yun, Sung-Nam Lee, Chel-Jong Choi, Structural, chemical and electrical properties of Au/La_2O_3/n-GaN MIS junction with a high-k lanthanum oxide insulating layer, Journal of Electronic Materials. 48, no. 7 (2019) 4217-4225. https://doi.org/10.1007/s11664-019-07193-8.
42. McCafferty, P. G., A. Sellai, P. Dawson, H. Elabd, Barrier characteristics of PtSip-Si Schottky diodes as determined from IVT measurements, Solid-State Electronics. 39, no. 4 (1996) 583-592. https://doi.org/10.1016/0038-1101(95)00162-X.
43. Hudait, Mantu Kumar, S. B. Krupanidhi, Effects of thin oxide in metal–semiconductor and metal–insulator–semiconductor epi-GaAs Schottky diodes, Solid-State Electronics. 44, no. 6 (2000) 1089-1097. https://doi.org/10.1016/S0038-1101(99)00320-2.
44. Zeyrek, Sedat, Ş. Altındal, H. Yüzer, Mehmet Mahir Bülbül, Current transport mechanism in Al/Si_3N_4/p-Si (MIS) Schottky barrier diodes at low temperatures, Applied Surface Science. 252, no. 8 (2006) 2999-3010. https://doi.org/10.1016/j.apsusc.2005.05.008.
45. Jyothi, I., V. Janardhanam, Hyobong Hong, Chel-Jong Choi, Current–voltage and capacitance–voltage characteristics of Al Schottky contacts to strained Si-on-insulator in the wide temperature range, Materials Science in Semiconductor Processing. 39 (2015) 390-399. https://doi.org/10.1016/j.mssp.2015.05.043.
46. Yıldırım, M. Ali, Betül Güzeldir, A. Ateş, Mustafa Sağlam, Temperature dependent current–voltage characteristics of the Zn/ZnO/n-Si/Au–Sb structure with ZnO interface layer grown on n-Si substrate by SILAR method, Microelectronic engineering 88, no. 10 (2011) 3075-3079. https://doi.org/10.1016/j.mee.2011.05.025.
47. Aldemir, D. Ali, M. Benhaliliba, C. E. Benouis, Photodiode based on Al-doped SnO_2: Fabrication, current-voltage and capacitance-conductance-voltage measurements, Optik. 222 (2020) 165487. https://doi.org/10.1016/j.ijleo.2020.165487.
48. Sze, Simon M., Yiming Li, Kwok K. Ng, Physics of semiconductor devices, John wiley & sons (2021).
49. Neamen, Donald A., Dhrubes Biswas, Semiconductor physics and devices, New York: McGraw-Hill higher education (2011).
50. Aiswarya, K. U., K. J. Arun, M. D. Aggarwal, and Padmaja Guggilla, A comprehensive review of suitable interfacial insulating layer selection, IV characteristics and working

parameters in MIS structured Schottky diodes for multifunctional optoelectronic applications, Discover Electronics. 3, no. 1 (2026) 66.
https://doi.org/10.1007/s44291-026-00216-9